

A new F_{ST} -based method to uncover local adaptation using environmental variables.

Pierre de Villemereuil* & Oscar E. Gaggiotti*†

*: Université Joseph Fourier, Centre National de la Recherche Scientifique,
LECA, UMR 5553, 2233 rue de la piscine, 38400 Saint Martin d'Hères, France

†Scottish Oceans Institute, University of St Andrews,
Fife, KY16 8LB, United Kingdom

Keywords: genome-scan, local adaptation, environment, F model, Bayesian methods, false discovery rate

Corresponding author: Pierre de Villemereuil, E-mail: bonamy@horus.ens.fr

Abstract

• Genome-scan methods are used for screening genome-wide patterns of DNA polymorphism to detect signatures of positive selection. There are two main types of methods: (i) “outlier” detection methods based on F_{ST} that detect loci with high differentiation compared to the rest of the genome, and (ii) environmental association methods that test the association between allele frequencies and environmental variables.

• We present a new F_{ST} -based genome-scan method, BayeScEnv, which incorporates environmental information in the form of “environmental differentiation”. It is based on the F model, but, as opposed to existing approaches, it considers two locus-specific effects; one due to divergent selection, and another due to various other processes different from local adaptation (e.g. range expansions, differences in mutation rates across loci or background selection). The method was developed in C++ and is available at <http://github.com/devillemereuil/bayescenv>.

• A simulation study shows that our method has a much lower false positive rate than an existing F_{ST} -based method, BayeScan, under a wide range of demographic scenarios. Although it has lower power, it leads to a better compromise between power and false positive rate.

• We apply our method to a human dataset and show that it can be used successfully to study local adaptation. We discuss its scope and compare it to other existing methods.

Introduction

One of the most important aims of population genomics (Luikart *et al.*, 2003) is to uncover signatures of selection in genomes of non model species. Of special interest is the process of local adaptation, whereby populations

20 experiencing different environmental conditions undergo adaptive, selective pressures specific to their local
21 habitat. As a result, populations evolve traits that provide an advantage in their local environment. Many
22 experimental approaches focused on potentially adaptive traits have been developed to test for local adaptation
23 (reviewed in Blanquart *et al.*, 2013), but only recently it has become possible to make inferences about the
24 genomic regions involved in local adaptation processes. Indeed, the advent of next generation sequencing (NGS,
25 Shendure and Ji, 2008) has fostered the development of so-called genome-scan methods aimed at identifying
26 regions of the genome subject to selection. These methods are now widely used in studies of local adaptation
27 (Faria *et al.*, 2014).

28 There are two main types of genome-scan methods. The first type detects ‘outlier’ loci using locus-specific
29 F_{ST} estimates, which are compared to either an empirical distribution (Akey *et al.*, 2002), or to a distribution
30 expected under a neutral model of evolution (Beaumont and Balding, 2004; Foll and Gaggiotti, 2008). The
31 rationale behind these methods is that local adaptation leads to strong genetic differentiation between popula-
32 tions, but only at the selected loci (or marker loci linked to them). Thus, loci with very high F_{ST} compared to
33 the rest of the genome are suspected to be under strong local adaptation and are referred to as outliers. The
34 outlier approach was further extended to statistics akin to F_{ST} (Bonhomme *et al.*, 2010; Günther and Coop,
35 2013), and also to other unrelated statistics (Duforet-Frebourg *et al.*, 2014). One limitation of these methods is
36 that they are not designed to test hypotheses about the environmental factors underlying the selective pressure.

37 A second type of methods focuses on environmental variables and aims at associating patterns of allele fre-
38 quency to environmental gradients. The rationale is that selective pressures should create associations between
39 allele frequencies at the selected loci and the causal environmental variables (Coop *et al.*, 2010). In the presence
40 of population structure, performing a simple linear regression would be an error-prone approach (De Mita *et al.*,
41 2013; de Villemereuil *et al.*, 2014). Instead, existing methods account for population structure by modelling
42 the allele frequency covariation across populations (Coop *et al.*, 2010; Frichot *et al.*, 2013; Guillot *et al.*, 2014).
43 One disadvantage of most of these approaches is that the parameters that capture the effect of demographic
44 history on genetic differentiation do not have a clear biological interpretation, which in turn makes the rejection
45 of the null model hard to interpret in terms of detection of local adaptation. Especially, note that although
46 the elements of the covariance matrix estimated by Coop *et al.* (2010) could in principle be interpreted as
47 parametric estimates of the pairwise and population-specific F_{ST} , this is only true when levels of genetic drift
48 are low (Nicholson *et al.*, 2002).

49 It is important to note that, regardless of the type of genome-scan method under consideration, processes
50 other than local adaptation might be responsible for the observed spatial patterns in allele frequency or F_{ST} .
51 These include demographic processes such as allele surfing (Edmonds *et al.*, 2004) or hierarchical population
52 structure (Excoffier *et al.*, 2009), large differences in mutation rate across loci (Edelaar *et al.*, 2011), hybrid
53 incompatibility following secondary contact (Kruuk *et al.*, 1999) and background selection (Charlesworth, 1998).

54 It is therefore possible that some of the loci identified as outliers are in fact false positives. Accounting for
55 processes other than selection would require introducing parameters that could appropriately capture the effect
56 of these other processes.

57 Here, we present a method that incorporates features of the two types of genome-scans described above.
58 The objective is to allow inferences about the environmental factors underlying selective pressures, and simul-
59 taneously better discriminate between true and false genetic signatures of local adaptation. Note that our new
60 method focuses only on local adaptation driven by a focal environmental variable and, therefore, differs from
61 other F_{ST} -based methods that carry out "blind" genome scans. Thus, this new approach is aimed at testing
62 hypothesis about specific drivers of local adaptation such as altitude (Bigham *et al.*, 2010; Foll *et al.*, 2014),
63 salinity (Larsson *et al.*, 2007; Daub *et al.*, 2013), pathogens (Fumagalli *et al.*, 2011; Daub *et al.*, 2013), etc.

64 Our method is based on the Bayesian approach first proposed by Beaumont and Balding (2004) and later
65 extended by Foll and Gaggiotti (2008). The original formulation considers population- and locus-specific F_{ST} 's,
66 which are described by a logistic model with three parameters: a locus-specific term, α_i , that captures the effect
67 of mutation and some forms of selection, a population-specific term, β_j , that captures demographic effects (e.g.
68 N_e and migration) and a locus-by-population interaction term, γ_{ij} , that reflects the effect of local adaptation.
69 The estimation of the first two terms benefits from sharing information across loci or populations, but this is
70 not the case for the interaction term, which is therefore poorly estimated (Beaumont and Balding, 2004, but
71 see Riebler *et al.*, 2008). In practice signatures of local adaptation are therefore inferred from the locus-specific
72 effects (α_i) under the assumption that large positive values reflect adaptive selection. The implicit assumption
73 is that background selection and mutation should not have much of an effect on this term. In order to relax this
74 assumption and to better estimate the interaction term we introduce environmental data so that $\gamma_{ij} = g_i E_j$,
75 where E_j is the "environmental differentiation" observed in population j and g_i is a locus-specific coefficient.
76 In what follows, we first describe in detail the probabilistic model underlying our Bayesian approach. We then
77 evaluate its performance using simulated data and then present an application using a human dataset. Finally,
78 we discuss the scope of our method and compare it with other existing genome-scan approaches.

79 **Statistical model**

80 **Modelling allele frequencies using the F model**

81 Our new genome-scan approach is based on the F model (Beaumont and Balding, 2004; Foll and Gaggiotti,
82 2008) and extends the software BayeScan (Foll and Gaggiotti, 2008) by incorporating environmental data so as
83 to explicitly consider local adaptation scenarios. Full details of the F model are given by Gaggiotti and Foll
84 (2010), so here we only provide a brief description. The core assumptions of the F model is that all populations
85 share a common pool of migrants, but that their effective sizes and immigration rates are population-specific.

86 Thus, population structure at each locus is described by local F_{ST} 's that measure genetic differentiation between
 87 each local population and the migrant pool.

88 The F model uses the multinomial-Dirichlet likelihood for the allele counts $\mathbf{a}_{ij} = (a_{ij1}, \dots, a_{ijK_i})$ at locus
 89 i within population j (where K_i is the number of distinct alleles at locus i) with parameters given by the
 90 migrant pool allele frequencies, $\mathbf{f}_i = (f_{i1}, \dots, f_{iK_i})$, and a population- and locus-specific parameter of similarity,
 91 $\theta_{ij} = \frac{1 - F_{ST}^{ij}}{F_{ST}^{ij}}$:

$$\mathbf{a}_{ij} \sim \text{multDir}(\theta_{ij}f_{i1}, \dots, \theta_{ij}f_{iK_i}), \quad (1)$$

92 where *multDir* stands for the multinomial-Dirichlet distribution.

93 Although, for the sake of simplicity, we only present here the formulation for co-dominant data, the software
 94 implementing our approach also allows for dominant data (e.g. AFLP markers) using the same probabilistic
 95 model as Foll and Gaggiotti (2008). Note finally that, for bi-allelic co-dominant markers (e.g. SNP markers),
 96 the likelihood reduces to a beta-binomial model.

97 **Alternative models to explain population structure**

98 Our purpose is to better discriminate between true signals of local adaptation and spurious signals left by other
 99 processes. Therefore, we assume that genetic differentiation at individual loci is influenced by three type of
 100 effects: (i) genome-wide effects due to demography, (ii) a locus-specific effect due to local adaptation caused by
 101 the focal environmental variable, and (iii) locus-specific effects unrelated to the focal environmental variable.
 102 Although in principle one could consider all seven alternative models that can be constructed with different
 103 combinations of these three effects, most of them would not have any biological meaning. For example, all
 104 models should include genome-wide effects associated with genetic drift. Additionally, we do not consider the
 105 two types of locus-specific effects simultaneously in a full model. The reason for this is that the inclusion of
 106 α_i along with g_i is not justified biologically. This is because the joint effect of local adaptation and another
 107 locus-specific effect such as allele surfing or background selection on the same locus is extremely unlikely either
 108 because of the strong effect of genetic drift in the first instance or the implausibility of a favourable variant
 109 arising and increasing in frequency in a highly conserved region subject to strong purifying selection. Thus, we
 110 focus on three different models to explain the genetic structuring at individual loci.

111 **Null model of population structure** Under the null hypothesis that all loci are neutral, the local differ-
 112 entiation parameter F_{ST}^{ij} will be driven only by local population demography and, hence, should be common to
 113 all loci:

$$\log \left(\frac{F_{ST}^{ij}}{1 - F_{ST}^{ij}} \right) = \log \left(\frac{1}{\theta_{ij}} \right) = \beta_j. \quad (2)$$

114 A high β_j value means that the population j is strongly differentiated from the pool of migrants. This could
 115 be due to a lack of immigration from the other populations, a reduced effective size, or a particular spatial

116 structure.

117 **Alternative model of local adaptation** In this model, we focus on a particular signature left by a process of
118 local adaptation. If selection is driven by a putative environmental factor, we expect that genetic differentiation
119 for the locus or loci under selection will be stronger than expected under neutrality for populations with strong
120 environmental differentiation. Any measure of distance between the environmental value of population j and
121 the average environment could serve as a measure of differentiation. For the sake of simplicity, we here only
122 consider the absolute value. Furthermore, in order to facilitate the calibration of prior distributions, we consider
123 standardised environmental values with unit variance.

124 To model the effect of local adaptation on locus i , we consider the impact of environmental differentiation E_j
125 of population j on the locus, we thus modify Eq. 2 as follows:

$$\log \left(\frac{F_{ST}^{ij}}{1 - F_{ST}^{ij}} \right) = \beta_j + g_i E_j, \quad (3)$$

126 where g_i quantifies the sensitivity of locus i to the environmental differentiation.

127 **Alternative model of locus-specific effect** Local adaptation with respect to the focal environmental
128 variable is not the only evolutionary phenomenon that could lead to departures from the neutral model. Other
129 phenomena that could produce such locus-specific effects include local adaptation due to other unknown factors,
130 large differences in mutation rate across loci, the so-called allele surfing phenomenon (Edmonds *et al.*, 2004)
131 and background selection (Charlesworth, 2013).

132 This is accounted for by using the following parametrisation for local differentiation:

$$\log \left(\frac{F_{ST}^{ij}}{1 - F_{ST}^{ij}} \right) = \alpha_i + \beta_j. \quad (4)$$

133 The main advantage of implementing both of the above alternative models is that we can distinguish between
134 departures from the neutral model of unknown origin (using Eq. 4) and departures due to local adaptation
135 caused by a particular environmental factor (using Eq. 3).

136 Material and Methods

137 Implementation of the statistical model

138 Our method, summarised in Fig. 1, uses two types of data: (i) the allele counts \mathbf{a} for each locus in each pop-
139 ulation sample, and (ii) observed values \mathbf{E} of an environmental variable (one value per population), which are
140 transformed into environmental differentiation using an appropriate function. Indeed, our model aims at asso-
141 ciating genetic distance (i.e. the F_{ST}^{ij}) with an environmental distance. Note that measuring an environmental

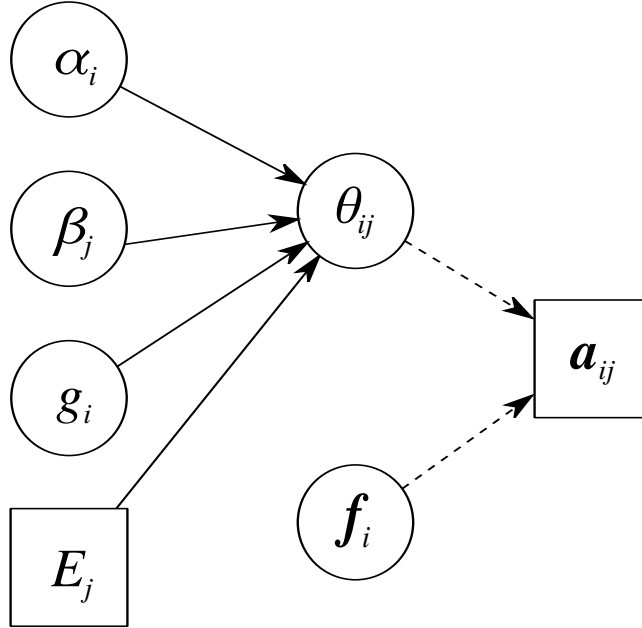


Figure 1: Directed Acyclic Graph (DAG) of the model. Squared nodes denote known quantities (E for environmental data, and A for genetic marker data). Circled nodes denote unknown parameters. Plain arrows stand for deterministic relationships, and dashed arrows stand for stochastic relationships.

142 distance requires to define a reference. The most natural reference would be the average of the environmental
 143 values, but this would not be always the case (see the example of adaptation to altitude in humans presented
 144 below). Also, it is strongly advised to standardise the environmental values by dividing by the standard deviation,
 145 in order to avoid effect size issues regarding the inference of the parameter g .

146 As stated in the previous section, there are three different models:

147 **M1** Neutral model: β_j ,

148 **M2** Local adaptation model with environmental differentiation E_j : $\beta_j + g_i E_j$,

149 **M3** Locus-specific model: $\alpha_i + \beta_j$.

150 Note that in our framework, the focal model being tested against the two others is **M2**. Thus, power and
 151 error rates (FPR and FDR) are computed for model **M2**. Model **M3** can be considered as a “nuisance model”
 152 whose role is to reduce the overall false positive rate by explaining the inflation of the variance in F_{ST} due
 153 to locus-specific effects other than selection driven by the focal environmental factor. Hence, the statistical
 154 significance of the parameter α_i is not of interest for BayeScEnv: only the significant values of g_i are considered.
 155 All three models were implemented using an RJMCMC algorithm (Green, 1995). In order to propose relevant
 156 values for new parameters during the jumps, the RJMCMC is preceded by pilot runs. These are aimed at
 157 both calibrating the MCMC proposals to reach efficient acceptance rates, and approximating the posterior
 158 distribution of parameters, as proposed by Brooks (1998) and already implemented in BayeScan (Foll and
 159 Gaggiotti, 2008). Our code is based on the source code of BayeScan 2.1 and is written in C++. The source

160 and binaries are available at <https://github.com/devillemereuil/bayescenv>.

161 Our prior belief in the three models is described by two parameters: the probability π of moving away from
162 the neutral model and the preference p for **M3** against **M2** as alternative models. We can calculate the prior
163 probability for each model as:

$$\begin{aligned} P(\mathbf{M1}) &= 1 - \pi, \\ P(\mathbf{M2}) &= \pi(1 - p), \\ P(\mathbf{M3}) &= \pi p. \end{aligned} \tag{5}$$

164 The mathematical details of the transition between models can be found in the Supplementary Material. Pilot
165 studies showed that using values of p above 0.5 yielded extremely conservative results (note that setting $p = 1$
166 would mean that model **M3** is always favoured over **M2**, in which case the power of the method is zero, yielding
167 no positives whatsoever).

168 We used a uniform Dirichlet prior for the allele frequencies $\mathbf{f}_i \sim Dir(1, \dots, 1)$. The priors for the hyperparamete-
169 rters α and β , were Normal with mean -1 and variance 1 (note that the results of our method will be especially
170 sensitive to the prior mean of α , but our pilot studies showed that -1 was a good default). Since under a local
171 adaptation scenario the parameter g is only expected to be positive, it was assigned a uniform prior between 0
172 and 10.

173 Our method outputs posterior error probabilities and q -values, which are test statistics related to the False
174 Discovery Rate (FDR) (Storey, 2002; Käll *et al.*, 2008). Contrary to the commonly used False Positive Rate
175 (FPR), which is the probability of declaring a locus as positive given that it is actually neutral, the FDR is the
176 proportion of the positive results that are in fact false positives, and is more appropriate for multiple testing
177 (Käll *et al.*, 2008). See the Supplementary Information (SI) for more details.

178 **Simulation analysis**

179 We performed a simulation study to evaluate the performance of our method and compare it with that of
180 BayeScan (Foll and Gaggiotti, 2008). We modelled 16 populations each with 500 individuals genotyped at 5,000
181 loci, among which one (monogenic scenario) or 50 (polygenic scenario) were under selection. We modelled three
182 kinds of population structure: *(i)* a classical island model (IM), *(ii)* a one-dimension stepping-stone (SS) model
183 and *(iii)* a hierarchically structured (HS) model.

184 The genome was composed of 5,000 bi-allelic SNPs spread along 10 chromosomes. The loci under selection due
185 to an environmental variable E (see Fig. S2 and Eq. S7 and S8), one for the monogenic case and 50 for the
186 polygenic case, were randomly distributed across the genome. Since all markers were independently initialised,
187 our simulations yielded negligible linkage disequilibrium. Consequently, we considered as true positives only
188 the loci subject to selection. For the IM and SS scenarios, we directly initialised all 16 populations. For the HS
189 scenario, we initialised the ancestral population, which, following successive and temporally spaced-out fission

190 events, gave rise to 2, 4, . . . , 16 populations. This hierarchical structure is reinforced by preferential migration
191 between related populations. More details regarding migration and population history are available in the SI.
192 This model is very close to that used by de Villemereuil *et al.* (2014). It should be particularly difficult for our
193 method, because all populations are equally differentiated (i.e. the β_j parameters are expected to be roughly
194 the same across populations), but a phylo-geographic covariance exists between related populations, which is
195 not explicitly accounted for by our probabilistic model. More information regarding the environmental gradient
196 and the fitness function are available in the SI, but, briefly, a polygenic multiplicative model was used with a
197 selection strength of 0.02 (0.1 for the monogenic case).

198 The simulations were performed using the SimuPOP Python library (Peng and Kimmel, 2005) and the scripts
199 are available online in the data section. Our simulated datasets were analysed using our C++ code and version
200 2.1 of BayeScan (Foll and Gaggiotti, 2008).

201 We generated 100 datasets for each scenario and computed the realised FDR, FPR and power yielded by BayeS-
202 can and our new environmental method (BayeScEnv). For the latter, we also compared several parametrisations
203 using a prior probability π of jumping away from the neutral model of 0.1 (equivalent to the default prior odds
204 used by BayeScan, which is 10) or 0.5, as well as a preference for the locus-specific model p of 0.5 (environ-
205 mental and locus-specific models are equiprobable) or 0 (the locus-specific model is forbidden and only the
206 environmental model is tested against the neutral one).

207 We supplemented these scenarios with a heterogeneous mutation rate case, based on the IM scenario above,
208 where most of the genome had a high mutation rate of 0.05, whereas 50 loci had a low mutation rate of 10^{-7} .
209 The result was an overall low F_{ST} of 0.05 for the whole genome, and of 0.10 for the low mutating loci.

210 **HGDP SNP data analysis**

211 In order to test our new method against a real dataset, we focused on 26 Asian populations from the Human
212 Genome Diversity Panel (HGDP) SNP Genotyping data. This data set consists of 660,918 SNP markers
213 genotyped using Illumina 650Y arrays. After cleaning the dataset from mitochondrial and sex-linked markers,
214 we removed all markers with minor allele frequency below 5%. This left us with a total of 446,117 SNPs. For
215 all populations, we obtained the following environmental variables from the BIOCLIM database: mean annual
216 temperature, precipitation, and altitudinal data. We ran separate BayeScEnv analysis for each variable and
217 compared the results with BayeScan (which doesn't use environmental variables). After standardisation of
218 the environmental variables, we computed environmental differentiation from the mean for temperature and
219 precipitation, and from the sea level for elevation. Gene ontology enrichment tests for the detected genes were
220 performed using the "SNP mode" of the Gowinda software (Kofler and Schlötterer, 2012). The prior odds for
221 BayeScan was 10 for this analysis. BayeScEnv prior parameters for this analysis were $\pi = 0.1$ and $p = 0.5$.

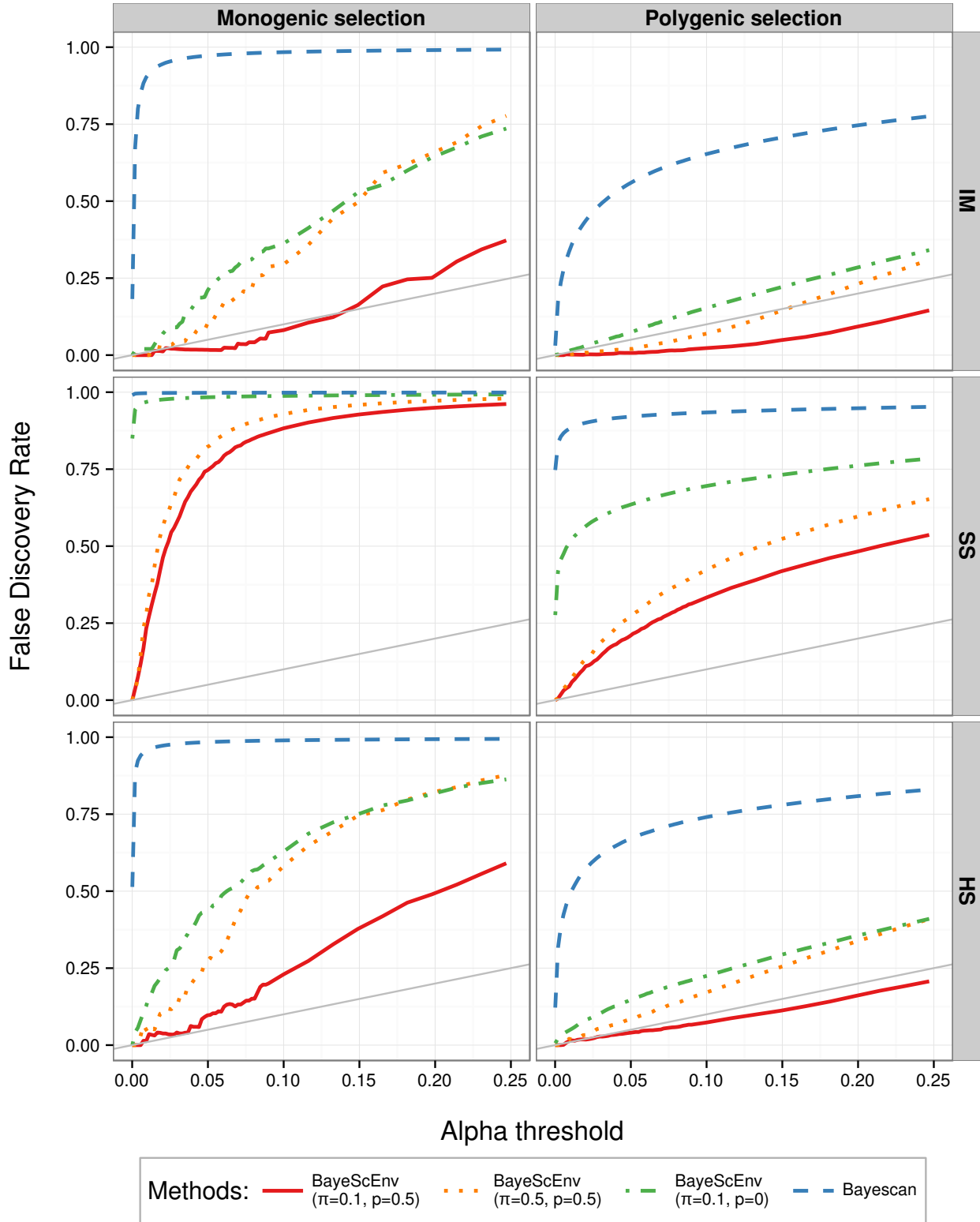


Figure 2: False Discovery Rate (FDR) against significance threshold α for three scenarios (IM: Island model, SS: Stepping-Stone model and HS: Hierarchically Structured model) and monogenic/polygenic selection. The grey line is the expected identity relationship between the FDR and α . The models tested are Bayescan (blue dashed), and BayeScEnv (orange dotted, green dot-dashed and solid red) with different probabilities π of jumping away from the neutral model (M1) and different preferences p for the locus-specific model (M3). Note that $p = 0$ means the environmental model (M2) is tested against the neutral one only.

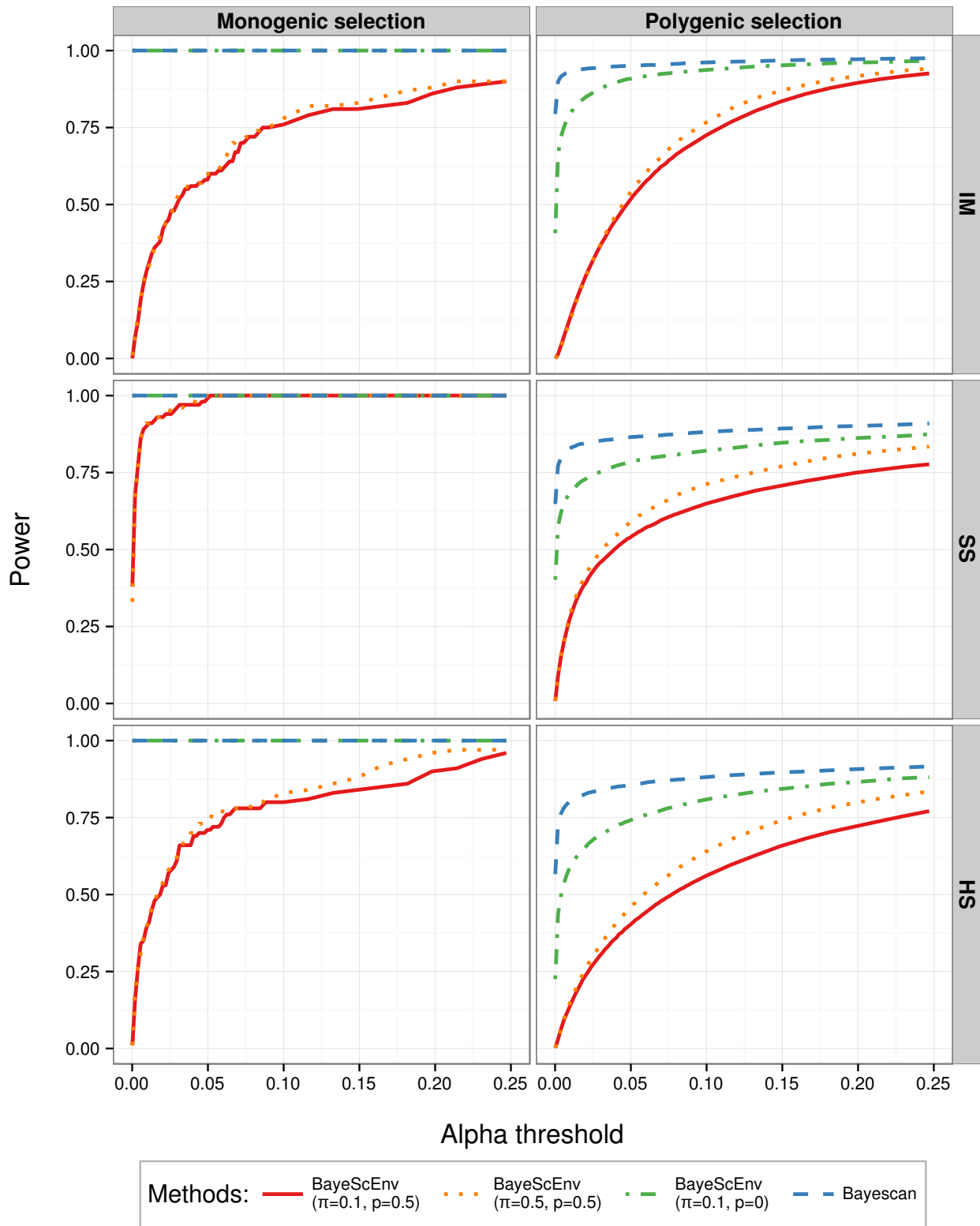


Figure 3: Power against significance threshold α for three scenarios (IM: Island model, SS: Stepping-Stone model and HS: Hierarchically Structured model) and monogenic/polygenic selection. The models tested are BayeScan (blue dashed), and BayeScEnv (orange dotted, green dot-dashed and solid red) with different probabilities π of jumping away from the neutral model (M1) and different preferences p for the locus-specific model (M3). Note that $p = 0$ means the environmental model (M2) is tested against the neutral one only.

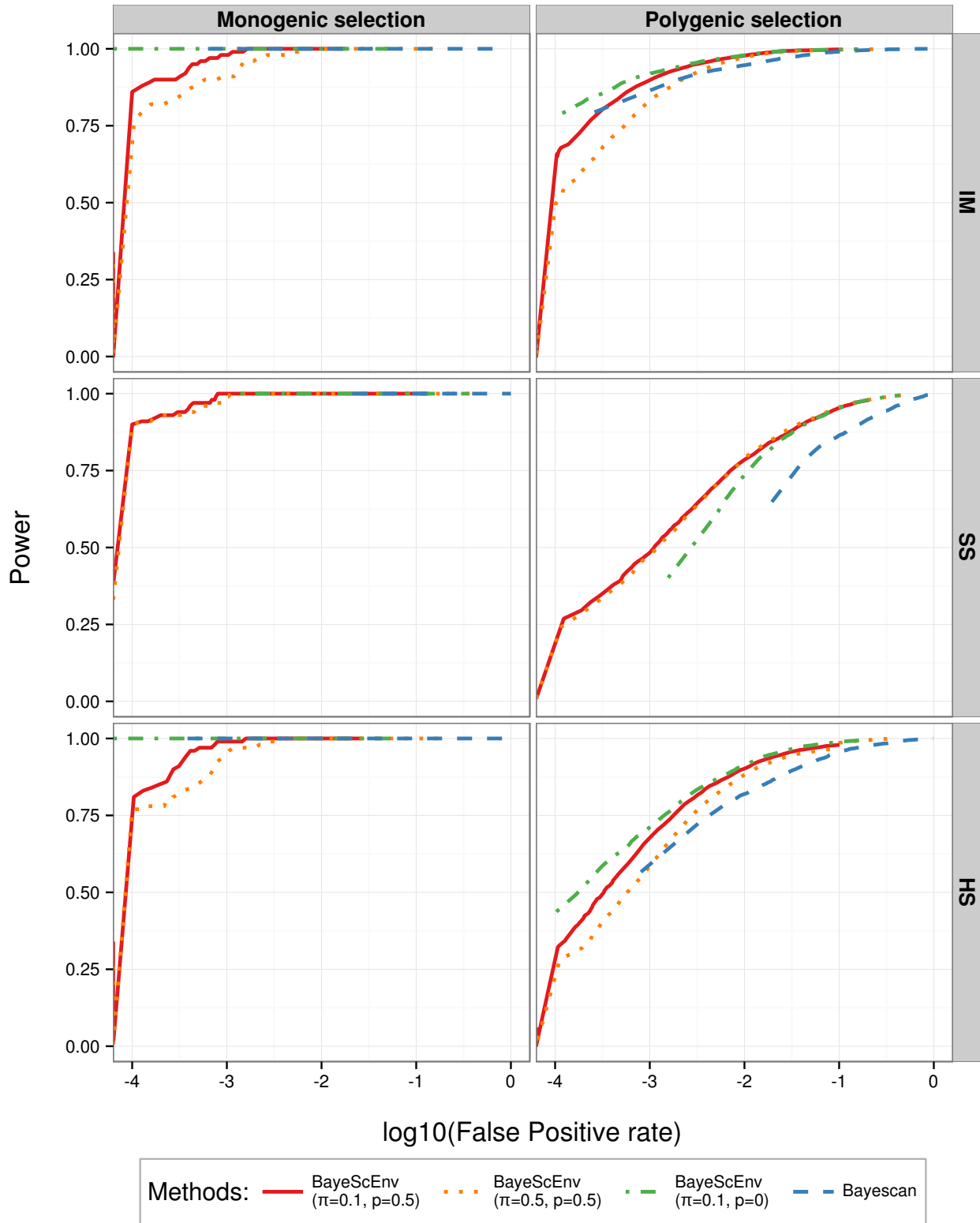


Figure 4: Power against False Positive Rate (FPR), a.k.a. ROC curve, for three scenarios (IM: Island model, SS: Stepping-Stone model and HS: Hierarchically Structured model) and monogenic/polygenic selection. The models tested are BayeScan (blue dashed), and BayeScEnv (orange dotted, green dot-dashed and solid red) with different probabilities π of jumping away from the neutral model (M1) and different preferences p for the locus-specific model (M3). Note that $p = 0$ means the environmental model (M2) is tested against the neutral one only.

222 Results

223 Simulation results

224 By definition, a threshold value of α used to decide whether q -values are significant or not is expected to yield
225 an FDR of α on the long run, when the model is robust and priors are calibrated. Recall that in BayeScEnv all
226 q -value tests below were performed on the parameter g to test for local adaptation. In the case of BayeScan,
227 on the other hand, the q -values correspond to parameter α .

228 As shown in Fig. 2, BayeScan was less well calibrated, yielding higher FDRs than BayeScEnv under all sce-
229 narios and for both monogenic and polygenic selection. Additionally, for BayeScEnv, the implementation using
230 $\pi = 0.1$ was fairly well calibrated (i.e. the curve is close the grey line in Fig. 2) under the IM scenario (for both
231 monogenic and polygenic versions) and under the polygenic version of the HS scenario. This implementation
232 was much more conservative than the one using $\pi = 0.5$. For $\pi = 0.1$ and $p = 0$, the FDRs were closer to those
233 yielded by BayeScan, but still lower.

234 The higher FDR for BayeScan and BayeScEnv with $\pi = 0.5$ or $p = 0$ was mainly driven by a higher FPR
235 rather than a lack of power (Fig. 3, see also Fig. S3 in the SI). Notably though, BayeScan had a quite high
236 power, higher than that of BayeScEnv. Note, however, that BayeScEnv with $p = 0$ had, as BayeScan, a maximal
237 power in the monogenic scenarios, and was almost as powerful as BayeScan in the polygenic scenarios. Yet
238 its FDR was lower (sometimes much lower) than that of BayeScan. This indicates that the incorporation of
239 environmental data helps to reduce the error rate both with or without the inclusion of spurious locus-specific
240 effects (α_i). More details regarding the FPR results are available in the Supplementary Information (Fig. S3).

241 Another traditional way to apprehend the compromise between power and false positives is the so-called
242 Receiver Operating Characteristics (ROC) curve, plotting power against FPR (Fig. 4). In these plots, the curve
243 that is “more to the left” is preferred because this means it offers higher power for a lower FPR. Fig. 4 shows
244 that BayeScEnv with $\pi = 0.1$ and $p = 0$ performed best under the IM and HS scenarios, whereas BayeScEnv
245 with $\pi = 0.1$ and $p = 0.5$ performed better under the “harder” SS scenario. Overall, although BayeScan has
246 higher power to detect local adaptation, it is still too liberal when deciding that a locus is under selection for
247 the scenarios we investigated.

248 The heterogeneous mutation scenario lead to a dramatically high false positive rate for the low mutating
249 loci in the case of Bayescan (62%). BayeScEnv, on the other hand, yielded a much lower false positive rate
250 for these loci (4.9%). Of course, because the higher differentiation due to low mutation rate can be seemingly
251 distributed according to the environmental variable, higher false positive rates will always be expected in such
252 a scenario. Nevertheless, BayeScEnv is an improvement over Bayescan in that regard.

Method	Variable	Nr of significant SNPs	Nr of significant GO terms	Nr of genes associated with a significant GO term
BayeScEnv	altitude	154	32	11
	temperature	170	103	20
	precipitation	2728	439	359
BayeScan	—	66,316	469	5628

Table 1: Results from BayeScan and BayeScEnv on the human dataset. FDR significance threshold was set to 5%. The total number of tested markers was 446,117.

253 Analysis of human data from Asia

254 The results of the human dataset analysis (Table 1) show a dramatic discrepancy between the two methods.
255 Whereas BayeScan yields a very large number (66,316) of markers considered as significant at the 5% threshold,
256 many fewer markers (154 to 2728) are considered significant by BayeScEnv. Gene Ontology (GO) enrichment
257 tests identified many significant terms (Table 1). Note, however, that in the altitude and temperature analyses
258 they correspond to a small number of genes (11 and 20 respectively, see Table 1). The number of genes is larger
259 for the precipitation analysis (359) and even larger for the analysis using BayeScan (5628).

260 Regarding the altitude, significant biological processes included the fatty acid metabolism (e.g. SCARB1),
261 skin pigmentation (e.g. MLANA, SLC24A5), kidney activity (e.g. SLC12A1) and oxido-reductase activity
262 (e.g. NOS1AP). Regarding the temperature, significant biological process included cardiac muscle activity (e.g.
263 SLC8A1) and development (e.g. NRG1, FOXP1), fatty acid metabolism (e.g. FADS1, FADS2) and response to
264 hypoxia (e.g. SLC8A1, SERPINA1). For the precipitation analysis with BayeScEnv, as well as the BayeScan
265 analysis, the number of significant terms was too large for hand-picked examples to be feasible.

266 The significance results (q -values) are displayed as a Manhattan plot in Fig. 5, along with the above
267 mentioned genes for the altitude and temperature analyses (Fig. 5, A and B). Other regions of the genome also
268 include outlier loci but they correspond to non-coding regions, or are close to genes associated to GO terms
269 that were not significant, or to proteins without a known function (e.g. C9orf91, which was the most significant
270 gene in the temperature analysis). Pattern of linkage disequilibrium was visible, which sometimes strongly
271 supported some candidate genes (Fig. 5, A, SLC12A1 and SLC24A5). Finally, comparing BayeScEnv (Fig. 5,
272 A, B and C) and BayeScan analyses (Fig. 5,D), we see that BayeScan yielded too many significant markers
273 for a Manhattan plot to be a useful display of the results. An interesting pattern is that BayeScan yielded
274 far more outlier markers with maximal certainty (e.g. posterior probability of one) than BayeScEnv. For the
275 present dataset, 22,516 markers had a posterior probability of one, whereas the maximal posterior probability
276 yielded by BayeScEnv was 0.9998. Finally, almost all loci detected using BayeScEnv were also found when using
277 BayeScan (between 98% for altitude to 100% for the two other variables).

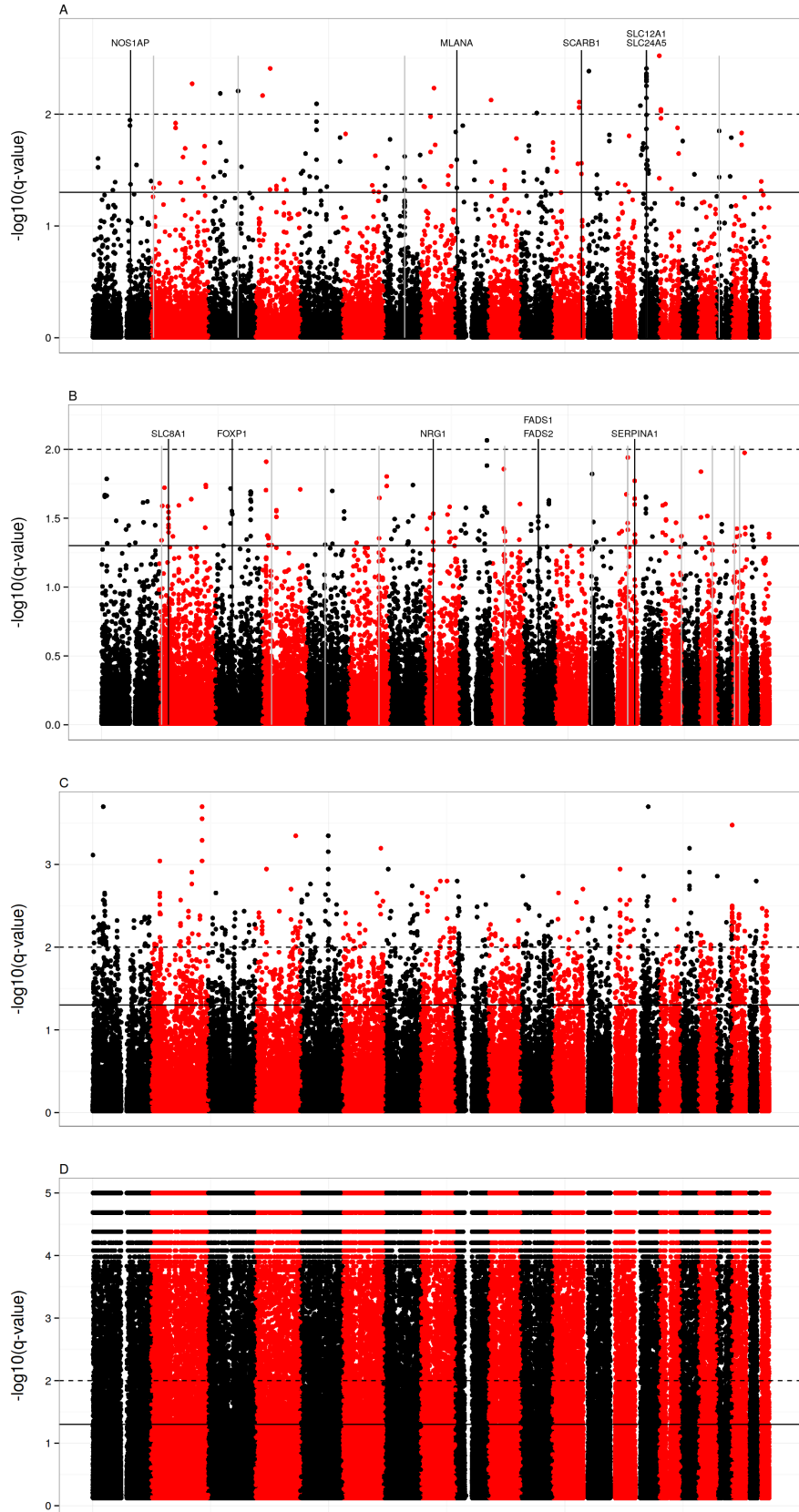


Figure 5: Manhattan plot of the q -values for the human dataset when using BayeScEnv with altitude (A), temperature (B), precipitations (C) or when using BayeScan (D). For altitude and temperature (A and B), genes mentioned in the text are displayed using black lines and genes associated with a significant GO term using grey lines. Top “stripes” for BayeScan (D) are artefacts due to finite number of iterations in RJMCMC (e.g. 0, 1, 2, 3... iterations outside of the non-neutral model), corresponding to determined posterior probabilities when divided by the total number of iterations. 14

278 Discussion

279 Features and performance of the method

280 The method we introduce in this paper, BayeScEnv, has several desirable features. First, just as BayeScan, it
281 is a model-based method. This means that the null model can be understood in terms of a process of neutral
282 evolution. One can thus predict what the method is able to fit or not. Second, we explicitly model a process
283 of local adaptation caused by an environmental variable. Third, in order to render the model more robust, we
284 account for locus-specific effects unrelated to the environmental variable under consideration. These departures
285 can be due to another process of local adaptation (i.e. caused by unknown environmental variables), to large
286 differences in mutation rates across loci, to background selection (Charlesworth, 2013) or complex spatial effects,
287 such as allele surfing (Edmonds *et al.*, 2004) and hierarchical population structure (Excoffier *et al.*, 2009). Our
288 simulation results show that when compared to BayeScan, BayeScEnv has a better control of its false discovery
289 rate under various scenarios (Fig. 2), yielding fewer, but more reliable candidate markers. Obviously, this has
290 a cost in terms of absolute power (Fig. 3), but BayeScEnv still performs better than BayeScan in terms of the
291 investigated compromises between true and false positives (i.e. FDR and ROC, Fig.2 & 4).

292 Besides, the parametrisation of BayeScEnv allows for a fine and intuitive control of the false positive rate
293 and power. For example, setting p to 0 increases both power and false positive rate, whereas setting $p = 0.5$
294 will allow for a more conservative test. This is because with $p = 0$, that is when the locus-specific effect model
295 (M3) is excluded, the local adaptation model (M2) will absorb much of the signal in the data, yielding a higher
296 probability of detecting true positives, but also a higher sensitivity to false positives. Our simulation results
297 show that, if the species under study has moderate to large dispersal abilities (c.f. hierarchical structure or island
298 model), the former parametrisation will be more appropriate, whereas for species with low dispersal abilities
299 (c.f. stepping-stone model) the latter should be preferred. Thus, being able to choose the right parametrisation
300 only requires limited knowledge about the dispersal abilities of the species.

301 We note that BayeScan was recently extended to consider species with hierarchical population structure
302 (BayeScan3, Foll *et al.*, 2014). With BayeScan3 it is now possible to study widely distributed species covering
303 several continents or geographic regions. It is also possible to better focus on local adaptation by considering
304 groups that include pairs of populations inhabiting different environments such as low and high altitude habitats.
305 Thus, BayeScan3, allows for the consideration of categorical environmental variables. Our new approach on the
306 other hand, allows the study of local adaptation related to continuous environmental variables in species with
307 a more restricted range.

308 **How to quantify ‘environmental differentiation’?**

309 To model local adaptation, we compute an “environmental differentiation” in terms of the distance (absolute
310 value) to a reference value. Although this reference can conveniently be chosen as the average of the environ-
311 mental values across the sampled populations, other kinds of reference may be biologically more relevant. For
312 example, in our analysis of the effect of elevation in humans, it seems appropriate to use sea level as the refer-
313 ence. Indeed, given the kind of environmental variables elevation is a proxy for (e.g. partial pressure of oxygen,
314 temperature, solar radiation, etc.), for most systems we would consider the sea level as a neutral environment
315 rather than the differentiated one.

316 Another way to account for environmental differentiation is to use Principal Component Analysis (PCA),
317 providing one of the axes to BayeScEnv as a description of the distance between environments. Despite this prac-
318 tice being an elegant way to summarise environmental distance between populations, it also has the drawback
319 of making it more difficult to identify the “causal” variable.

320 Note that the environmental variables must be standardised so as to avoid scale inconsistencies between g
321 and α and β . If we choose the average environmental value as reference, then standardisation involves mean-
322 centring and rescaling to have unit variance. However, if we choose another reference, then standardisation only
323 involves rescaling to have unit variance.

324 Finally, the software implementation of our method only accepts one environmental variable at the time
325 as including more than one variable would considerably slow the algorithm down, and render the biological
326 interpretation of g quite tedious. Also, when using several correlated variables, it is important to realise that
327 statistically distinguishing between the relative selective roles of each one would require many populations.

328 **Comparison with other environmental association methods**

329 There are several genome-scan approaches that incorporate environmental information, such as Bayenv (Coop
330 *et al.*, 2010), LFMM (Frichot *et al.*, 2013) and gINLAnd (Guillot *et al.*, 2014). These methods perform a
331 regression between allele frequencies and environmental values. Yet non-equilibrium situations combined with
332 complex spatial structuring can lead to spatial correlations in allele frequencies, which in turn can lead to high
333 false positive rates. To minimise this problem, the above methods take into account allele frequency correlations
334 across populations while performing the regression.

335 BayeScEnv, on the other hand, assumes that all populations are independent, exchanging genes only through
336 the migrant pool. However, it includes a locus-specific effect unrelated to the environmental variable that helps
337 to take into account locus-specific spatial effects due to deviations from the underlying demographic model. The
338 fact that this approach works is illustrated by our simulation study, which showed that BayeScEnv was fairly
339 robust to isolation-by-distance and a hierarchically structured scenario. Moreover, the analyses of simulated
340 datasets from de Villemereuil *et al.* (2014), available in the SI, show that even under very complex scenarios,

341 BayeScEnv can compete with other environmental association methods. In particular, most of these scenarios
342 assume an environmental selective gradient confounded with population structure, which is particularly hard
343 for genome scan methods (Frichot *et al.*, 2015): the results show that, in that case, BayeScEnv suffer from low
344 power, but not from an excess of false positives. When compared with the other methods (including Bayenv
345 and LFMM), BayeScEnv typically yields a medium FDR for most scenarios, and is less scenario-sensitive than
346 Bayenv and LFMM. Nevertheless, we note that BayeScEnv is best suited for species with medium to high
347 dispersal abilities such as marine species and anemophilous plants.

348 Another point that distinguishes BayeScEnv from these methods is that it does not assume any particu-
349 lar functional form for the relationship between environmental values and allele frequencies. While existing
350 association methods all assume a clinal pattern, BayeScEnv only assumes that genetic differentiation increase
351 exponentially with environmental differentiation. This allows for a more diverse family of relationships between
352 allele frequencies and the environment.

353 Finally, BayeScEnv is one of the very few methods to study gene-environment associations that can be used
354 with dominant data (but see also Guillot *et al.*, 2014).

355 **Data analysis**

356 When confronted with real datasets, BayeScEnv typically returned fewer significant markers than BayeScan.
357 This is explained both by the focus on searching for outliers linked to a specific environmental factor and by
358 the lower false positive rate of our approach. When applied to the human dataset, BayeScEnv identified several
359 genomic regions that are enriched for gene ontology terms relevant to potential local adaptation to altitude
360 or temperature. We emphasise that this study was not meant to exhaustively and rigorously investigate local
361 adaptation in Asian human populations. However, our results tend to demonstrate that the candidates yielded
362 by BayeScEnv have a biological interpretation. For example, skin pigmentation and cardiac activity could
363 clearly be involved in responses to increased solar radiation and depleted oxygen availability at high elevation.

364 Much of the ontologies linked to temperature were potentially confounded with adaptation to altitude, such
365 as the response to hypoxia and cardiac muscle activity. Also, fatty acid metabolism was associated to both
366 altitude and temperature. Of course, the biological functions described here do not account for all the signals
367 yielded by BayeScEnv (see Fig. 5, A and B). Other genomic significant regions include genes with less obvious
368 biological function regarding local adaptation, non-coding regions and proteins without a known function.
369 Finally, the analysis using the precipitation variable yielded too many significant markers for a detailed analysis
370 of the biological functions involved. This may not necessarily be due to a confounding effect of the spatial
371 structure (the human Asian populations being structured mainly from West to East, while the Eastern climate
372 is characterised by strong precipitations during the monsoon), since precipitation may behave as a surrogate
373 for several environmental variables.

374 Conclusion

375 The main improvement introduced by our new method, BayeScEnv, over existing F_{ST} -based genome-scan
376 approaches is the possibility of focusing on the detection of outlier loci linked to genomic regions involved
377 in local adaptation and better distinguishing between the signal of positive selection and that of other locus-
378 specific processes such as mutation (see the heterogeneous mutation rate scenario in the Results) and background
379 selection. Although it does not explicitly model complex spatial effects, the consideration of two different locus-
380 specific effects make it more robust to potential deviations from the migrant pool model. This is reflected in its
381 much lower false discovery rate when compared to BayeScan.

382 Our new formulation also allows for an improved control of the true/false positives compromise through
383 the parameter p , which describes our preference for the model that includes a locus-specific effect unrelated to
384 the environmental factor over the model that includes environmental effects. Although we recommend using
385 $p = 0.5$, lower values (including 0) could be used if population structure is weak or maximising power is more
386 important than reducing the false positive rate.

387 With this new method, there are now three alternative formulations of genome-scan methods based on the
388 F model. BayeScan detects a wide range of locus-specific effects (including background selection). Although
389 its false discovery rate is higher than that of the two extensions, it is able to detect regions of the genome
390 subject to purifying selection. The hierarchical version of this original formulation, BayeScan3, allows the
391 study of local adaptation due to categorical environmental factors. Finally, our new method, BayeScEnv, is
392 more appropriate to detect genomic regions under the influence of selective pressures exerted by continuous
393 environmental variables. Thus, all three methods are complementary and jointly cover scenarios applicable to
394 a wide range of species

395 Acknowledgement

396 We thank M. Foll for providing the source code of BayeScan and for clarifying several issues related to the code,
397 J. Renaud for his help on getting the average altitude out of the HGDP latitude/longitude data, S. Schoville
398 for the BIOCLIM data, E. Bazin for his help on the HGDP data analysis. PdV was supported by a doctoral
399 studentship from the French *Ministère de la Recherche et de l'Enseignement Supérieur*. OEG was supported
400 by the Marine Alliance for Science and Technology for Scotland (MASTS).

401 References

402 Akey JM, Zhang G, Zhang K, Jin L, Shriver MD (2002) Interrogating a High-Density SNP Map for Signatures
403 of Natural Selection. *Genome Research*, **12**(12), 1805–1814.

404 Beaumont MA, Balding DJ (2004) Identifying adaptive genetic divergence among populations from genome
405 scans. *Molecular Ecology*, **13**(4), 969–980.

406 Bigham A, Bauchet M, Pinto D, Mao X, Akey JM, Mei R, Scherer SW, Julian CG, Wilson MJ, López Herráez D,
407 Brutsaert T, Parra EJ, Moore LG, Shriver MD (2010) Identifying Signatures of Natural Selection in Tibetan
408 and Andean Populations Using Dense Genome Scan Data. *PLoS Genet*, **6**(9), e1001116.

409 Blanquart F, Kaltz O, Nuismer SL, Gandon S (2013) A practical guide to measuring local adaptation. *Ecology*
410 *Letters*, **16**(9), 1195–1205.

411 Bonhomme M, Chevalet C, Servin B, Boitard S, Abdallah J, Blott S, SanCristobal M (2010) Detecting selection
412 in population trees: the Lewontin and Krakauer test extended. *Genetics*, **186**(1), 241–262.

413 Brooks S (1998) Markov chain Monte Carlo method and its application. *Journal of the Royal Statistical Society:*
414 *Series D (The Statistician)*, **47**(1), 69–100.

415 Charlesworth B (1998) Measures of divergence between populations and the effect of forces that reduce vari-
416 ability. *Molecular Biology and Evolution*, **15**(5), 538–543.

417 Charlesworth B (2013) Background Selection 20 Years on: The Wilhelmine E. Key 2012 Invitational Lecture.
418 *Journal of Heredity*, **104**(2), 161–171.

419 Coop G, Witonsky D, Di Rienzo A, Pritchard JK (2010) Using Environmental Correlations to Identify Loci
420 Underlying Local Adaptation. *Genetics*, **185**(4), 1411–1423.

421 Daub JT, Hofer T, Cutivet E, Dupanloup I, Quintana-Murci L, Robinson-Rechavi M, Excoffier L (2013) Evi-
422 dence for Polygenic Adaptation to Pathogens in the Human Genome. *Molecular Biology and Evolution*, **30**(7),
423 1544–1558.

424 De Mita S, Thuillet AC, Gay L, Ahmadi N, Manel S, Ronfort J, Vigouroux Y (2013) Detecting selection
425 along environmental gradients: analysis of eight methods and their effectiveness for outbreeding and selfing
426 populations. *Molecular Ecology*, **22**(5), 1383–1399.

427 Duforet-Frebourg N, Bazin E, Blum MGB (2014) Genome Scans for Detecting Footprints of Local Adaptation
428 Using a Bayesian Factor Model. *Molecular Biology and Evolution*, **31**(9), 2483–2495.

429 Edelaar P, Burraco P, Gomez-Mestre I (2011) Comparisons between QST and FST—how wrong have we been?
430 *Molecular Ecology*, **20**(23), 4830–4839.

431 Edmonds CA, Lillie AS, Cavalli-Sforza LL (2004) Mutations arising in the wave front of an expanding population.
432 *Proceedings of the National Academy of Sciences of the United States of America*, **101**(4), 975–979.

- 433 Excoffier L, Hofer T, Foll M (2009) Detecting loci under selection in a hierarchically structured population.
434 *Heredity*, **103**(4), 285–298.
- 435 Faria R, Renaut S, Galindo J, Pinho C, Melo-Ferreira J, Melo M, Jones F, Salzburger W, Schluter D, Butlin R
436 (2014) Advances in Ecological Speciation: an integrative approach. *Molecular Ecology*, **23**(3), 513–521.
- 437 Foll M, Gaggiotti OE (2008) A Genome-Scan Method to Identify Selected Loci Appropriate for Both Dominant
438 and Codominant Markers: A Bayesian Perspective. *Genetics*, **180**(2), 977–993.
- 439 Foll M, Gaggiotti OE, Daub JT, Vatsiou A, Excoffier L (2014) Widespread Signals of Convergent Adaptation
440 to High Altitude in Asia and America. *The American Journal of Human Genetics*, **95**(4), 394–407.
- 441 Frichot E, Schoville SD, Bouchard G, François O (2013) Testing for Associations between Loci and Environ-
442 mental Gradients Using Latent Factor Mixed Models. *Molecular Biology and Evolution*, **30**(7), 1687–1699.
- 443 Frichot E, Schoville SD, de Villemereuil P, Gaggiotti OE, François O (2015) Detecting adaptive evolution based
444 on association with ecological gradients: Orientation matters! *Heredity*.
- 445 Fumagalli M, Sironi M, Pozzoli U, Ferrer-Admettla A, Pattini L, Nielsen R (2011) Signatures of Environmental
446 Genetic Adaptation Pinpoint Pathogens as the Main Selective Pressure through Human Evolution. *PLoS*
447 *Genet*, **7**(11), e1002355.
- 448 Gaggiotti OE, Foll M (2010) Quantifying population structure using the F-model. *Molecular Ecology Resources*,
449 **10**(5), 821–830.
- 450 Green PJ (1995) Reversible jump Markov chain Monte Carlo computation and Bayesian model determination.
451 *Biometrika*, **82**(4), 711–732.
- 452 Guillot G, Vitalis R, Rouzic AI, Gautier M (2014) Detecting correlation between allele frequencies and environ-
453 mental variables as a signature of selection. A fast computational approach for genome-wide studies. *Spatial*
454 *Statistics*, **8**, 145–155.
- 455 Günther T, Coop G (2013) Robust Identification of Local Adaptation from Allele Frequencies. *Genetics*, **195**(1),
456 205–220.
- 457 Kofler R, Schlötterer C (2012) Gowinda: unbiased analysis of gene set enrichment for genome-wide association
458 studies. *Bioinformatics*, **28**(15), 2084–2085.
- 459 Kruuk LEB, Baird SJE, Gale KS, Barton NH (1999) A comparison of multilocus clines maintained by environ-
460 mental adaptation or by selection against hybrids. *Genetics*, **153**(4), 1959–1971.
- 461 Käll L, Storey JD, MacCoss MJ, Noble WS (2008) Posterior Error Probabilities and False Discovery Rates:
462 Two Sides of the Same Coin. *Journal of Proteome Research*, **7**(1), 40–44.

- 463 Larsson LC, Laikre L, Palm S, André C, Carvalho GR, Ryman N (2007) Concordance of allozyme and mi-
464 crosatellite differentiation in a marine fish, but evidence of selection at a microsatellite locus. *Molecular*
465 *Ecology*, **16**(6), 1135–1147.
- 466 Luikart G, England PR, Tallmon D, Jordan S, Taberlet P (2003) The power and promise of population genomics:
467 from genotyping to genome typing. *Nature Reviews Genetics*, **4**(12), 981–994.
- 468 Nicholson G, Smith AV, Jónsson F, Gústafsson O, Stefánsson K, Donnelly P (2002) Assessing Population
469 Differentiation and Isolation from Single-Nucleotide Polymorphism Data. *Journal of the Royal Statistical*
470 *Society. Series B (Statistical Methodology)*, **64**(4), 695–715.
- 471 Peng B, Kimmel M (2005) simuPOP: a forward-time population genetics simulation environment. *Bioinformat-*
472 *ics*, **21**(18), 3686–3687.
- 473 Riebler A, Held L, Stephan W (2008) Bayesian Variable Selection for Detecting Adaptive Genomic Differences
474 Among Populations. *Genetics*, **178**(3), 1817–1829.
- 475 Shendure J, Ji H (2008) Next-generation DNA sequencing. *Nature Biotechnology*, **26**(10), 1135–1145.
- 476 Storey JD (2002) A direct approach to false discovery rates. *Journal of the Royal Statistical Society: Series B*
477 *(Statistical Methodology)*, **64**(3), 479–498.
- 478 de Villemereuil P, Frichot E, Bazin E, François O, Gaggiotti OE (2014) Genome scan methods against more
479 complex models: when and how much should we trust them? *Molecular Ecology*, **23**(8), 2006–2019.

480 **Data Accessibility**

481 The Python code used to simulate data is available online in the Supplementary Information. The software
482 and its source code are available online at GitHub: <http://github.com/devillemereuil/bayescenv>. The
483 HGDP dataset is available at <http://www.hagsc.org/hgdp/files.html>. The BIOCLIM database is available
484 at <http://worldclim.org/bioclim>.

485 **Author contributions**

486 PdV and OEG designed the statistical model. PdV modified the C++ code and performed the simulation and
487 data analysis. PdV and OEG wrote the article.